IEEE Access
Multidisciplinary | Rapid Review | Open Access Journal

Received March 26, 2020, accepted April 9, 2020, date of publication April 14, 2020, date of current version April 30, 2020.

*Digital Object Identifier 10.1109/ACCESS.2020.2987914*

# Quaternion Discrete Fourier Transform-Based Color Image Watermarking Method Using Quaternion QR Decomposition

**MIANJIE LI[1], (Graduate Student Member, IEEE), XIAOCHEN YUAN[1,2], (Member, IEEE), HAI CHEN[3], AND JIANQING LI[1], (Senior Member, IEEE)**

[1]Faculty of Information Technology, Macau University of Science and Technology, Taipa, Macau
[2]Zhuhai M.U.S.T. Science Research Academy, Zhuhai 519000, China
[3]Information Science and Technology, Beijing Normal University, Zhuhai 519000, China

Corresponding author: Xiaochen Yuan (xcyuan@must.edu.mo)

This work was supported in part by the National Natural Science Foundation of China under Grant 61902448, and in part by the Science and Technology Development Fund of Macau Special Administrative Region (SAR) under Grant 0007/2018/ASC.

**ABSTRACT** In this paper, a new Quaternion Discrete Fourier Transform (QDFT)-based digital color image watermarking method is presented. In addition, the Quaternion QR (QQR) decomposition is applied in digital watermarking technology for the first time. First of all, the QDFT and QQR decomposition are performed on the host image, respectively, to acquire the scalar part of the quaternion matrix for watermark information embedding. After that, we divide the scalar part of the quaternion matrix generated by the QQR decomposition into blocks and calculate the entropy. The block with high entropy is selected to embed the watermark information. Then the watermark information is embedded into the extracted block using the quantization index modulation method. We conducted a large number of tests and experimental results indicate that the presented approach obtains excellent robustness against Scaling, Rotation, Median filtering, 'Salt & Pepper' noise, and JPEG Compression. Compared with the existing methods, the presented method achieves better performance.

**INDEX TERMS** Watermarking technology, quaternion discrete Fourier transform (QDFT), quaternion QR (QQR) decomposition, quantization index modulation, scalar part.

## I. INTRODUCTION

Currently, it is becoming easier to modify digital multimedia content, especially in terms of images. Therefore, image copyright protection has become more and more concerned. Digital image watermarking technology is widely used to alleviate this problem. According to the information required for digital watermark information extraction, we classify the digital image watermarking technology as non-blind, semi-blind and blind. The non-blind technology needs at least the host image when detecting information. It can detect information from the host image by the method of probability statistics. The semi-blind technology does not need the host image when detecting watermark information; however, it needs watermark information. Generally, the method of probability statistics is used to judge the existence of watermark information. The blind technology does not need the host image and the original watermark information when detecting watermark information. The non-blind technique and semi-blind technique need host image or the original watermark information, which brings inconvenience to the detection. Therefore, this paper studies the blind watermarking technique.

According to embedding region of the watermark information, we classify the digital image watermarking technology as spatial domain and transform domain. The spatial domain watermarking technology is to embed watermark information directly in the signal space. This technique is simple to implement, but it has less information embedded and poor robustness. The transform domain watermarking technology is to transform the image before embedding the watermark information and embed the watermark information by

The associate editor coordinating the review of this manuscript and approving it for publication was Mehul S Raval.

modifying some coefficients of the transform domain. The transform domain watermarking technology is helpful to improve imperceptibility. Although the computational complexity of the transform domain watermarking technique is larger than that of the spatial domain, it can provide better embedding capacity and robustness under various attacks [1]. Therefore, we explore the frequency domain-based watermarking method in this paper.

In recent years, many watermarking methods have been presented [1]–[22]. The existing methods mainly include the following types: Discrete Wavelet Transform (DWT) [1]–[3], [11], [12], Discrete Fourier Transform (DFT) [10], Discrete Cosine Transform (DCT) [6]–[9], Quaternion Discrete Fourier Transform (QDFT) [13], [15], [16], and Quaternion Hadamard Transform (QHT) [14]. Chou and Liu [11] presented a novel color image watermarking algorithm based on wavelet transform and just-noticeable difference, and the algorithm achieved better imperceptibility. Besides the method of processing the R, G, and B single channels, in color image watermarking, to perform joint processing by R, G, and B channels transform into quaternion is also possible. In [17], binary watermark information was inserted into the coefficients of the QDFT, and the color channels were not separated by quaternion transformation of the image. Ma *et al.* [19] presented invariant feature transform-based image watermarking method. The information was hidden in the quaternion matrix of the block with each invariant feature point as the center. Xia *et al.* [20] presented quaternion polar harmonic transforms-based digital watermarking method using chaotic system. Yang *et al.* [21] presented quaternion exponential moment-based digital watermarking method using least squares support vector machine. The disadvantage of that method was more expenses in calculation. Wang *et al.* [16] suggested the novel watermarking algorithm combining QDFT, LS-SVM, and pseudo Zernike moments. The color image performs the quaternion transformation, which allows the embedded information energy to be propagated to all channels at the same time, instead of just to one channel. Therefore, we presented QDFT-based color image watermarking scheme using QQR decomposition. The proposed watermarking scheme achieves satisfactory performance in terms of imperceptibility and robustness.

The rest of this paper is arranged as below. The proposed method is described in Section 2, including QDFT, QQR decomposition, and the embedding and extraction process of watermark. The experimental part is provided in Section 3. Finally, we summarize the paper in Section 4.

## II. PROPOSED QUATERNION TRANSFORM-BASED WATERMARKING

To improve the robustness of the presented watermarking scheme for color images, we perform information embedding on the quaternion matrix. The QDFT and QQR decomposition are 4D vector spaces that provide better performance than single channel transforms techniques such as DCT and DWT, and they are more suitable for RGB images. Therefore, we apply QDFT and QQR decomposition to RGB images and embed the watermark information to the scalar part of quaternion matrix by the QIM method. Next. We introduce QDFT, QQR decomposition, and watermark information embedding and extraction procedures.

### A. QUATERNION DISCRETE FOURIER TRANSFORM (QDFT)

Usually, a color host image has three channels, R, G, and B. The quaternion of each pixel can be expressed as:

$$Q(\alpha,\ \delta) = a + b(\alpha,\ \delta)\sigma + c(\alpha,\ \delta)\varsigma + d(\alpha,\ \delta)\tau \quad (1)$$

The conjugate and the modulus are given in the following (2) and (3) respectively:

$$Q(\alpha,\ \delta)^* = a - b(\alpha,\ \delta)\sigma - c(\alpha,\ \delta)\varsigma - d(\alpha,\ \delta)\tau \quad (2)$$

$$|Q(\alpha,\ \delta)| = \sqrt{a^2 + b^2(\alpha,\ \delta) + c^2(\alpha,\ \delta) + d^2(\alpha,\ \delta)} \quad (3)$$

where $\sigma^2 = \varsigma^2 = \tau^2 = -1$, $\sigma\varsigma = -\varsigma\sigma = \tau$, $\tau\sigma = -\sigma\tau = \varsigma$, $\varsigma\tau = -\tau\varsigma = \sigma$. $a = 0$, $b(\alpha,\ \delta)$, $c(\alpha,\ \delta)$, and $d(\alpha,\ \delta)$ correspond to R, G, and B values in color host image respectively.

Therefore, the color image is converted into quaternion matrix through quaternion transformation. To suppress the color distortion caused by embedding the watermark information, the color host image is transformed by the QDFT. The QDFT of the color host image produces coefficients that contain features of all channels of the image. Therefore, the coefficients generated by QDFT are used to embed the watermark information, and the watermark information will be distributed in each channel of the image. In this paper, we apply this feature of quaternion transformation to achieve better invisibility. The QDFT used in this paper is the left-side. The two-dimensional left-side QDFT and inverse transform are respectively defined below.

$$F(u,\ v) = \frac{1}{\sqrt{XY}} \sum_{\alpha=0}^{X-1} \sum_{\delta=0}^{Y-1} e^{-\mu 2\pi\left(\frac{\alpha u}{M} + \frac{\delta v}{N}\right)} Q(\alpha,\ \delta) \quad (4)$$

$$Q(\alpha,\ \delta) = \frac{1}{\sqrt{XY}} \sum_{u=0}^{X-1} \sum_{v=0}^{Y-1} e^{\mu 2\pi\left(\frac{\alpha u}{M} + \frac{\delta v}{N}\right)} F(u,\ v) \quad (5)$$

where $\mu^2 = -1$, $\mu$ is unit pure quaternion, $X \times Y$ is size of the color image.

### B. QUATERNION QR DECOMPOSITION (QQR DECOMPOSITION)

After the QDFT on the host image, we perform the QQR decomposition on the obtained QDFT coefficient $F(u,\ v)$. The QQR decomposition was developed by Bunse-Gerstner *et al.* [23] Each quaternion matrix can be decomposed into a multiplication of the unitary matrix and the upper triangular matrix. The QQR decomposition described herein maintains a quaternion structure before and after processing the QDFT coefficient $F(u,\ v)$.

In this paper, QDFT coefficient $F(u,\ v) \in \mathbf{H}^{n\times n}$, $\mathbf{H}^{n\times n}$ is defined as a quaternion matrix of $n \times n$. We set

$F(u,\ v)_0 := F(u,\ v)$. The following iterations are run when $k = 0,\ 1,\ 2,\ 3,\ \cdots$.

$$\begin{aligned} Factor\ F_k(u,\ v) &= Q_k R_k \\ SetF_{k+1}(u,\ v) &:= R_k Q_k \\ F_{k+1}(u,\ v) &= Q_k^H F_k Q_k \end{aligned} \tag{6}$$

Let $E$ be the permutation matrix and let a circumflex denote the $2n$-by-$2n$ representation of a quaternion matrix. The following formula can be obtained.

$$\begin{aligned} E\hat{F}_k(u,\ v)E^H &= (E\hat{Q}_k E^H)(E\hat{R}_k E^H) \\ E\hat{F}_{k+1}(u,\ v)E^H &= (E\hat{R}_k E^H)(E\hat{Q}_k E^H) \end{aligned} \tag{7}$$

where $E\hat{Q}_k E^H$ and $E\hat{R}_k E^H$ are unitary matrix and triangular matrix, respectively. The scalar part of $E\hat{F}_k(u,\ v)E^H$ acquired by decomposing coefficients of QDFT has an even symmetry property. In order to make the inverse transformed matrix still a pure quaternion matrix to guarantee imperceptibility, we embed information into the scalar part of the upper triangular matrix.

### C. PROCEDURES OF WATERMARK EMBEDDING

Figure 1 shows the detailed flowchart of embedding watermark. First, the QDFT and QQR decomposition discussed above are used to acquire scalar part for watermark information embedding. In our method, the scalar part is blocked by size of 128 × 128, and then we will calculate the entropy value for each block and select the block with high entropy for watermarking. Next, we apply the QIM method to embed each watermark bit into extracted block, as mentioned in the Figure 1. After the watermark information is embedded and the watermarked block is generated, the corresponding block in the scalar part is replaced with its corresponding watermarked block to generate a watermarked scalar part. Finally, we apply watermarked scalar part replacement, inverse QDFT and QQR decomposition to reconstruct the watermarked image. The embedding process of watermark information is as below.

**STEP-1** Performs QDFT and QQR decomposition on the color image, and then we select the upper triangular matrix in the obtained matrix. As shown in sections II. A and II. B.

**STEP-2** Extract the scalar part of the upper triangular matrix for embedding watermark information.

**STEP-3** Divides the scalar part of size 512 × 512 into a plurality of blocks of size 128 × 128 and calculates an entropy value for each of the blocks, thereby selecting a block of high entropy to form the watermark information embedding block.

**STEP-4** Inserts each bit of the watermark information wm into the block of the high entropy of the selected scalar part, as below:

$$I'(\alpha,\delta) = \begin{cases} 2\varphi \times round(I(\alpha,\delta)/2\varphi) + \varphi/2 & wm(i,j) = 1 \\ 2\varphi \times round(I(\alpha,\delta)/2\varphi) - \varphi/2 & wm(i,j) = 0 \end{cases} \tag{8}$$

where $I(\alpha,\ \delta)$ represents scalar part of the upper triangular matrix in location$(\alpha,\ \delta)$, $wm(i,\ j)$ corresponds to watermark bit, $round(\ )$ is rounding operator, and $\varphi$ denotes the quantization step.

**STEP-5** The watermarked scalar part can be generated by replacing the block in the corresponding scalar part with a watermarked block.

**STEP-6** The watermarked upper triangular matrix can be generated by replacing the scalar part in the corresponding matrix with a watermarked scalar part.

**STEP-7** Apply inverse QQR decomposition and QDFT to reconstruct the watermarked image.

### D. PROCEDURES OF WATERMARK EXTRACTION

Figure 2 illustrates the process of extracting the watermark. Above all, rotation angle estimation and correction are performed on the received image before watermark information extraction. Then, the QDFT and QQR decomposition are executed to acquire upper triangular matrix. The scalar part of the upper triangular matrix is then selected to perform watermark information extraction. The process of extracting watermark information is as below.

**STEP-1** Perform rotation angle estimation and correction. To estimate the rotation angle, the binarization is applied to the received image and the radon transform is then accordingly applied; in this way, the rotation angle of the obtained image can be calculated by using the deviation distance of the image edge point. Reference [24] With the estimated angle, the received image can be anti-rotated to its regular position.

**STEP-2** Performs the QDFT and QQR decomposition on the received color image, and then we select the upper triangular matrix in the obtained unitary matrix and the upper triangular matrix.

**STEP-3** Extract the scalar part of the upper triangular matrix for extracting watermark information.

**STEP-4** Divides the scalar part of size 512 × 512 into multiple blocks of size 128 × 128 and calculates the entropy value for each of the blocks, and select the block with high entropy to extract the watermark information.

**STEP-5** Extracts each bit of watermark information from the block with high entropy of the scalar part by formula (9), as follows:

$$wm(i,\ j)' = \begin{cases} 1 & I(\alpha,\ \delta)' - 2\varphi \cdot round(I(\alpha,\ \delta)'/2\varphi) > 0 \\ 0 & I(\alpha,\ \delta)' - 2\varphi \cdot round(I(\alpha,\ \delta)'/2\varphi) \le 0 \end{cases} \tag{9}$$

where $wm(i,\ j)'$ denotes the extracted watermark bit, $I(\alpha,\ \delta)'$ represents the received scalar part of upper triangular matrix in location $(\alpha,\ \delta)$, and $\varphi$ denotes the quantization step decrypted by the keys.

## III. EXPERIMENTAL RESULTS AND DISCUSSIONS

We have shown the performance of this method through a series of experiments, and only representative experimental results are given herein. In this paper, MATLAB R2018b is used as the experimental platform. In addition, the step size was set to 1050 in subsequent experiments.

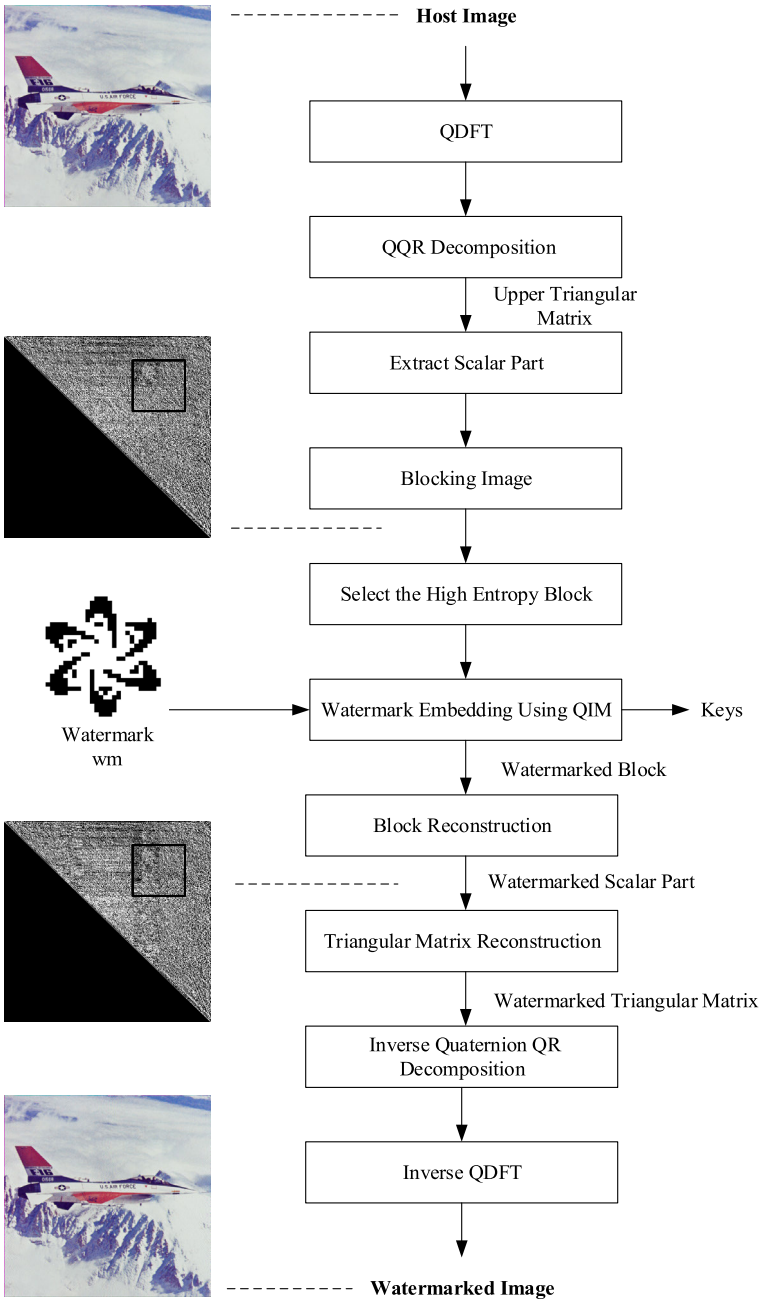


**FIGURE 1.** Flowchart for embedding watermark.

The difference in quality between original and watermarked images is evaluated using the Peak Signal-to-Noise Ratio (PSNR) and the Structural Similarity Index (SSIM). The larger PSNR or SSIM means better perceived quality. The Bit Error Rate (BER) and Normalized Correlation (NC) were calculated for measuring robustness. The smaller BER value or larger NC value, the stronger robustness. The calculation formulas of PSNR, SSIM, BER, and NC are shown in formula (10) - (13). Figure 3 (a)-(e) show some test color images and binary watermark image. Figure 4(a)-(e) show the corresponding images with watermark and the extracted watermark image. The image size we tested is 512 × 512. The size of the watermark image is 32 × 32. We get average PSNR and SSIM values of 34 and 0.9906, respectively. In addition, the PSNR and SSIM values for the test image with the size of 1024 × 1024 are 47.0705 and 0.9995, respectively.

$$PSNR = 10\log_{10}\left(3XY \times 255^2 \Big/ \sum_{t=1}^{3}\sum_{r=1}^{X}\sum_{s=1}^{Y}\left[h(r,s,t) - h'(r,s,t)\right]^2\right) \quad (10)$$

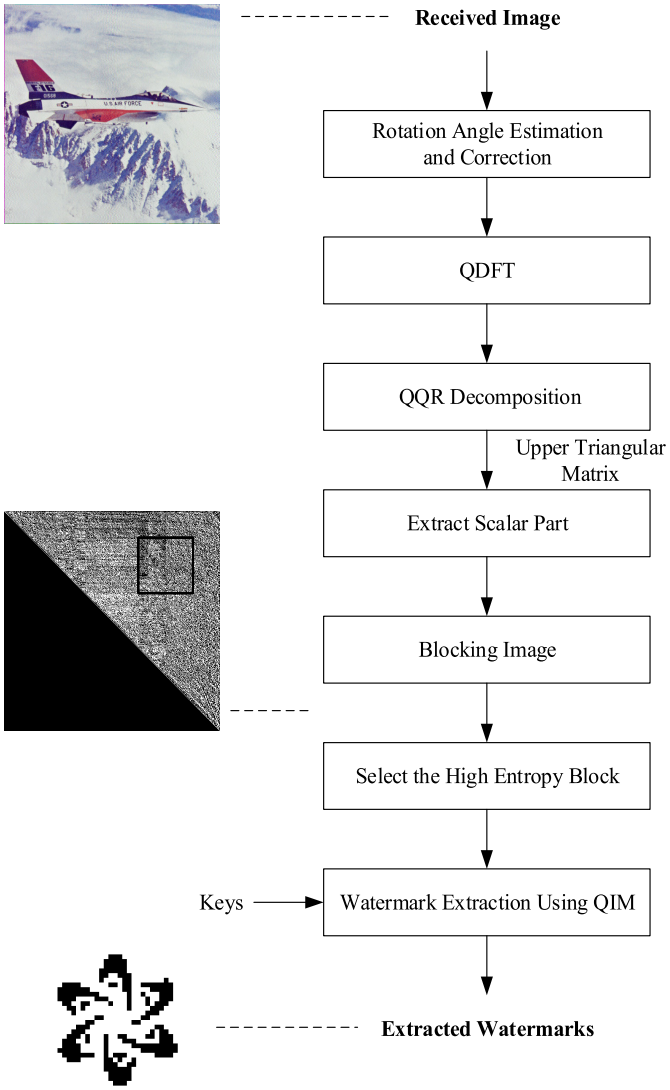


**FIGURE 2.** Flowchart for extracting watermark.

where $h$ represents pixel value of test image, $h'$ represents pixel value of image with watermark, and $X \times Y$ represents image size we tested.

$$SSIM(I, I') = \frac{(2\mu_I\mu_{\tilde{I}} + C_1)(2\sigma_{I\tilde{I}} + C_2)}{(\mu_I^2 + \mu_{\tilde{I}}^2 + C_1)(\sigma_I^2 + \sigma_{\tilde{I}}^2 + C_2)} \quad (11)$$

where $I$ and $I'$ denote the original host color image and the corresponding watermarked image respectively; $\mu_I$ and $\mu_{I'}$ are the average values of $I$ and $I'$, respectively; $\sigma_I^2$ and $\sigma_{I'}^2$ are the variances of $I$ and $I'$, respectively; $\sigma_{II'}$ is the covariance of $I$ and $I'$; $C_1$ and $C_2$ are the two variables to stabilize the division with the weak denominator.

$$BER = \frac{1}{V \times W} \sum_{x=1}^{V} \sum_{y=1}^{W} \begin{cases} 1, & wm'(i,j) \neq wm(i,j) \\ 0, & wm'(i,j) = wm(i,j) \end{cases} \quad (12)$$

where $wm'(i,j)$ represents extracted watermark, $wm(i,j)$ represents original watermark, and $V \times W$ represents watermark image size we used.

$$NC = \sum_{i=1}^{M} \sum_{j=1}^{N} wm'(i,j) \cdot wm(i,j) \cdot \frac{1}{\sum_{i=1}^{M} \sum_{j=1}^{N} [wm(i,j)]^2} \quad (13)$$

where $wm'(i,j)$ represents extracted watermark and $wm(i,j)$ is the original watermark image of size $M \times N$.

We perform a series of attacks and display the experimental results in TABLE 1. The various attacks and extracted watermark images are shown in TABLE 1. Besides the extracted watermark image, the calculated BER value is also given. The results suggest that our proposed scheme is strong robustness against various attacks.

Next, the experimental results of the presented method and the existing method [8], [14], [25] are compared. In Table 2 , we show the watermarked image quality comparison between

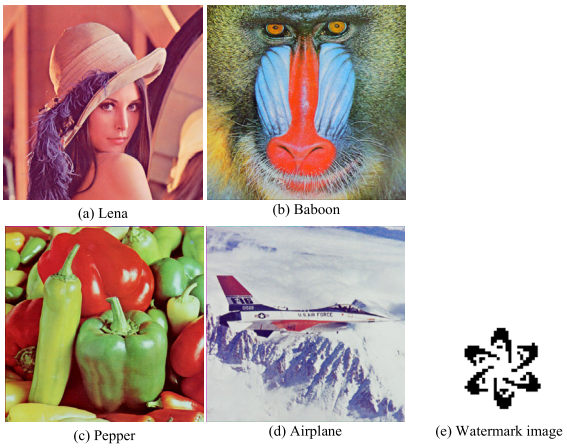


**FIGURE 3.** Original test color images and the watermark image.

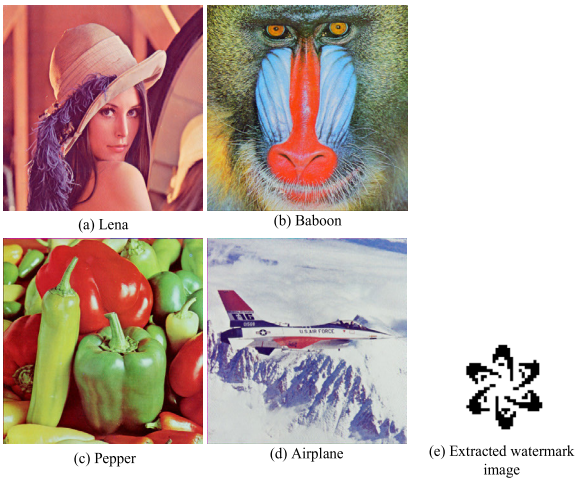


**FIGURE 4.** Corresponding images with watermark and extracted watermark image.

our scheme and the existing scheme. The average SSIM value we obtained is 0.9906, which is slightly better than the average SSIM values of 0.9893, 0.9897, and 0.9609 in [8], [14], and [25], respectively.

After that, we simulated the same attack technique: 'Salt & Pepper' noise with noise density of 0.01 and 0.02, $3 \times 3$ Median filtering, JPEG Compression with quality factor of 90, Scaling of 1.6 and 4, Rotation of $10^{\circ}$, and Cropping of 20% and 25%. Specifically, TABLE 3 and TABLE 4 show the BER and NC values detected by the presented approach and the existing approach. The best experimental results are shown in bold. In TABLE 3, Li *et al.* [14] presented QHT-based image watermarking algorithm. This algorithm used QHT to process the color image, and then embedded the watermark information by Schur decomposition and revising the Q matrix. Su *et al.* [8] presented a watermarking algorithm based on DC coefficients and distribution characteristics. The algorithm embedded watermark information by modifying pixel values in the spatial domain. In TABLE 4, Su [25] presented Hessenberg decomposition-based image

**TABLE 1.** The results of the extraction under various attacks.

| Attack | Lena | Peppers | Baboon |
|---|---|---|---|
| Contrast adjustment | 0.0137 | 0.0234 | 0.0146 |
| Histogram equalization | 0.0293 | 0.0400 | 0.0361 |
| Gamma Correction | 0.0137 | 0.0195 | 0.0166 |
| Brighten 1.2 | 0.0186 | 0.0166 | 0.0166 |
| Darken 0.8 | 0.0186 | 0.0098 | 0.0137 |
| Sharpening | 0.2930 | 0.3418 | 0.3340 |
| Gaussian Low pass filter 30 | 0.0107 | 0.0156 | 0.0176 |
| Butterworth High pass filter 10 | 0.0156 | 0.0127 | 0.0117 |
| Median filtering 3x3 | 0 | 0 | 0 |
| Salt & pepper noise 0.01 | 0.0146 | 0.0068 | 0 |
| Gaussian noise 0.001 | 0.0098 | 0.0117 | 0.0146 |
| Cropping 20% | 0.1631 | 0.1729 | 0.1602 |
| JPEG 90 | 0.0010 | 0.0010 | 0 |
| JPEG 70 | 0.0010 | 0 | 0 |
| JPEG 40 | 0.0098 | 0.0107 | 0.0117 |
| Rotation 10 | 0.0011 | 0.0013 | 0.0010 |
| Scaling 1.6 | 0.0020 | 0 | 0.0010 |
| Rotation 10 + Scaling 1.6 | 0.0127 | 0.0186 | 0.0215 |

**TABLE 2.** Compare the watermarked image quality of the presented scheme and existing scheme [8], [14], [25] in terms of SSIM.

| Scheme | SSIM |
|---|---|
| Scheme of [8] | 0.9893 |
| Scheme of [14] | 0.9897 |
| Scheme of [25] | 0.9609 |
| Presented scheme | **0.9906** |

watermarking algorithm. The watermark information was embedded into the orthogonal matrix of the Heisenberg decomposition of the color image. Compared with the existing methods, we applied the QQR decomposition to the digital watermark field for the first time. The proposed method applies QDFT and QQR decomposition to RGB color images and uses the QIM method to embed the watermark information into the scalar part of the quaternion matrix. Thereby, the robustness to common attack techniques and

**TABLE 3.** Compare the extracted results of the presented scheme and existing schemes [8], [14] in terms of NC.

| Attack | Lena | | | Peppers | | | Baboon | | |
|---|---|---|---|---|---|---|---|---|---|
| | Scheme of [14] | Scheme of [8] | Our | Scheme of [14] | Scheme of [8] | Our | Scheme of [14] | Scheme of [8] | Our |
| No attack | 1 | 1 | ***1*** | 1 | 0.9930 | ***1*** | 1 | 1 | ***1*** |
| Median filtering 3x3 | 0.8811 | 0.9674 | ***1*** | 0.8162 | 0.9683 | ***1*** | 0.7647 | 0.9965 | ***1*** |
| Salt & pepper noise 0.01 | 0.9396 | 0.9378 | ***0.9907*** | 0.9228 | 0.9257 | ***0.9956*** | 0.9450 | 0.9413 | ***1*** |
| Cropping 20% | **0.9910** | 0.9846 | *0.8918* | **0.9847** | 0.9820 | *0.8843* | 0.9865 | **0.9901** | *0.8938* |
| JPEG 90% | 0.9955 | 0.9985 | ***0.9983*** | 0.9604 | 0.9885 | ***0.9983*** | 0.9775 | 0.9980 | ***1*** |
| Rotation 10° | 0.9596 | / | ***0.9961*** | 0.9491 | / | ***0.9926*** | 0.9333 | / | ***0.9983*** |
| Scaling 1.6 | 0.9640 | / | ***0.9988*** | 0.9258 | / | ***1*** | 0.8964 | / | ***0.9983*** |

/ indicate that the result was not provided

**TABLE 4.** Compare the extracted results of the presented scheme and existing scheme [25] in terms of NC.

| Attack | Scheme of [25] | Our |
|---|---|---|
| JPEG 90% | 0.9678 | ***1*** |
| Scaling 4 | 0.9655 | ***1*** |
| Median filter 3 × 3 | 0.9363 | ***1*** |
| Cropping 25% | 0.9254 | *0.7059* |
| Salt & pepper noise 0.02 | 0.9896 | *0.9339* |

**TABLE 5.** Compare the extracted results of the presented scheme and existing scheme [13], [26], [27] in terms of NC.

| Attack | Scheme of [13] | Scheme of [26] | Scheme of [27] | Our |
|---|---|---|---|---|
| Salt & pepper noise 0.01 | 0.8954 | 0.8239 | 0.9186 | **0.9277** |
| Gaussian noise 0.005 | 0.8413 | 0.7310 | 0.8704 | **0.8789** |
| Median filter 3x3 | 0.7507 | 0.8507 | 0.9831 | **0.9961** |
| Average filter 3×3 | 0.7956 | 0.7956 | 0.9426 | **0.9766** |
| Gaussian filter 3x3 | 0.8364 | 0.8112 | 0.8514 | **0.9473** |
| JPEG 80 | 0.9331 | **0.9999** | 0.8538 | 0.9570 |
| Cropping 1/3 | 0.8036 | 0.7754 | **0.8570** | 0.7617 |
| Cropping 2/3 | 0.6523 | 0.6266 | **0.7032** | 0.6934 |
| Scale 0.9 | **1** | 0.9917 | 0.9334 | **1** |

the imperceptibility of watermark information are improved. The above analysis is verified by comparing the results. In TABLE 3, the proposed method has better performance advantages than the existing method under Scaling, Rotation, Median filtering, 'Salt & Pepper' noise, and JPEG Compression. However, the robustness against the Cropping attack is slightly worse than the comparison method. We will work on a local watermarking scheme to solve this problem in future work. In addition, the results of TABLE 4 can also be seen that experimental results of presented scheme are superior to the other schemes.

In order to further measure the performance of the proposed watermarking method, we compared the proposed method with the existing method [13], [26], [27] in Table 5. To make a fair comparison, the PSNR values of all watermarked images are controlled at 40 dB by adaptively adjusting the embedding strength for all the methods. The experimental results show that the proposed method has satisfactory performance compared with the existing methods.

## IV. CONCLUSION

In this paper, we propose a color image watermarking method based on QDFT and QQR decomposition. The scalar part of the quaternion matrix generated by QQR decomposition, which is first applied to digital watermarking technology, is divided into blocks and the entropy value of each block is calculated. The block with high entropy is selected to embed and extract the watermark. In this work, The QDFT and QQR decomposition are 4D vector spaces that provide better performance than single channel transforms techniques such as DCT and DWT, and they are more suitable for color image. The color image pixel is taken as a quaternion vector, the quaternion transformation is performed on it, and then the watermark information is embedded into the frequency component. This allows the watermark information energy to propagate simultaneously to three channels instead of only to one channel. Therefore, the proposed method achieves a good trade-off between imperceptibility and robustness. According to the experimental results, the superiority of the proposed

method is illustrated by comparison with the existing state-of-the-art methods.

## REFERENCES

[1] C.-C. Lai and C.-C. Tsai, "Digital image watermarking using discrete wavelet transform and singular value decomposition," *IEEE Trans. Instrum. Meas.*, vol. 59, no. 11, pp. 3060–3063, Nov. 2010.
[2] D. Bhowmik, M. Oakes, and C. Abhayaratne, "Visual attention-based image watermarking," *IEEE Access*, vol. 4, pp. 8002–8018, 2016.
[3] Y. Tan, J. Qin, X. Xiang, W. Ma, W. Pan, and N. N. Xiong, "A robust watermarking scheme in YCbCr color space based on channel coding," *IEEE Access*, vol. 7, pp. 25026–25036, 2019.
[4] X.-Y. Wang, S.-Y. Zhang, T.-T. Wen, H. Xu, and H.-Y. Yang, "Synchronization correction-based robust digital image watermarking approach using Bessel K-form PDF," *Pattern Anal. Appl.*, 2019, doi: 10.1007/s10044-019-00828-w.
[5] N. Muhammad, N. Bibi, I. Qasim, A. Jahangir, and Z. Mahmood, "Digital watermarking using Hall property image decomposition method," *Pattern Anal. Appl.*, vol. 21, no. 4, pp. 997–1012, Nov. 2018.
[6] N. A. Loan, N. N. Hurrah, S. A. Parah, J. W. Lee, J. A. Sheikh, and G. M. Bhat, "Secure and robust digital image watermarking using coefficient differencing and chaotic encryption," *IEEE Access*, vol. 6, pp. 19876–19897, 2018.
[7] M. Barni, F. Bartolini, and A. Piva, "Multichannel watermarking of color images," *IEEE Trans. Circuits Syst. Video Technol.*, vol. 12, no. 3, pp. 142–156, Mar. 2002.
[8] Q. Su, Y. Niu, Q. Wang, and G. Sheng, "A blind color image watermarking based on DC component in the spatial domain," *Optik*, vol. 124, no. 23, pp. 6255–6260, Dec. 2013.
[9] S. Roy and A. K. Pal, "A blind DCT based color watermarking algorithm for embedding multiple watermarks," *AEU-Int. J. Electron. Commun.*, vol. 72, pp. 149–161, Feb. 2017.
[10] T. Kin Tsui, X.-P. Zhang, and D. Androutsos, "Color image watermarking using the spatio-chromatic Fourier transform," in *Proc. IEEE Int. Conf. Acoust. Speed Signal Process.*, vol. 2, 2006, p. 2.
[11] C.-H. Chou and K.-C. Liu, "A perceptually tuned watermarking scheme for color images," *IEEE Trans. Image Process.*, vol. 19, no. 11, pp. 2966–2982, Nov. 2010.
[12] S. M. M. Rahman, M. O. Ahmad, and M. N. S. Swamy, "A new statistical detector for DWT-based additive image watermarking using the Gauss–Hermite expansion," *IEEE Trans. Image Process.*, vol. 18, no. 8, pp. 1782–1796, Aug. 2009.
[13] B. Chen, G. Coatrieux, G. Chen, X. Sun, J. L. Coatrieux, and H. Shu, "Full 4-D quaternion discrete Fourier transform based watermarking for color images," *Digit. Signal Process.*, vol. 28, pp. 106–119, May 2014.
[14] J. Li, C. Yu, B. B. Gupta, and X. Ren, "Color image watermarking scheme based on quaternion Hadamard transform and Schur decomposition," *Multimedia Tools Appl.*, vol. 77, no. 4, pp. 4545–4561, Feb. 2018.
[15] C. Wang, X. Wang, C. Zhang, and Z. Xia, "Geometric correction based color image watermarking using fuzzy least squares support vector machine and bessel k form distribution," *Signal Process.*, vol. 134, pp. 197–208, May 2017.
[16] X.-Y. Wang, C.-P. Wang, H.-Y. Yang, and P.-P. Niu, "A robust blind color image watermarking in quaternion Fourier transform domain," *J. Syst. Softw.*, vol. 86, no. 2, pp. 255–277, Feb. 2013.
[17] P. Bas, N. Le Bihan, and J.-M. Chassery, "Color image watermarking using quaternion Fourier transform," in *Proc. IEEE Int. Conf. Acoust., Speech, Signal Process. (ICASSP)*, vol. 3, 2003, p. III-521.
[18] K. Prabha, M. J. Vaishnavi, and I. S. Sam, "Quaternion Hadamard transform and QR decomposition based robust color image watermarking," in *Proc. 3rd Int. Conf. Trends Electron. Informat. (ICOEI)*, Apr. 2019, pp. 101–106.
[19] X. Ma, Y. Xu, L. Song, X. Yang, and H. Burkhardt, "Color image watermarking using local quaternion Fourier spectral analysis," in *Proc. IEEE Int. Conf. Multimedia Expo*, Jun. 2008, pp. 233–236.
[20] Z. Xia, X. Wang, W. Zhou, R. Li, C. Wang, and C. Zhang, "Color medical image lossless watermarking using chaotic system and accurate quaternion polar harmonic transforms," *Signal Process.*, vol. 157, pp. 108–118, Apr. 2019.
[21] H.-Y. Yang, Y. Zhang, P. Wang, X.-Y. Wang, and C.-P. Wang, "A geometric correction based robust color image watermarking scheme using quaternion exponent moments," *Optik*, vol. 125, no. 16, pp. 4456–4469, Aug. 2014.
[22] I. Orović, P. Zogović, N. Žarić, and S. Stanković, "Speech signals protection via logo watermarking based on the time–frequency analysis," *Ann. Telecommun. Annales des télécommunications*, vol. 63, nos. 7–8, pp. 369–377, Aug. 2008.
[23] A. Bunse-Gerstner, R. Byers, and V. Mehrmann, "A quaternion QR algorithm," *Numerische Math.*, vol. 55, no. 1, pp. 83–95, Jan. 1989.
[24] E. T. Quinto, "The invertibility of rotation invariant radon transforms," *J. Math. Anal. Appl.*, vol. 91, no. 2, pp. 510–522, Feb. 1983.
[25] Q. Su, "Novel blind colour image watermarking technique using Hessenberg decomposition," *IET Image Process.*, vol. 10, no. 11, pp. 817–829, Nov. 2016.
[26] C. Das, S. Panigrahi, V. K. Sharma, and K. K. Mahapatra, "A novel blind robust image watermarking in DCT domain using inter-block coefficient correlation," *AEU-Int. J. Electron. Commun.*, vol. 68, no. 3, pp. 244–253, Mar. 2014.
[27] H. Xu, G. Jiang, M. Yu, and T. Luo, "A color image watermarking based on tensor analysis," *IEEE Access*, vol. 6, pp. 51500–51514, 2018.

**MIANJIE LI** (Graduate Student Member, IEEE) is currently pursuing the Ph.D. degree in electronic information technology with the Macau University of Science and Technology, Macau, China. His research interests include digital multimedia processing and digital watermarking.

**XIAOCHEN YUAN** (Member, IEEE) received the B.Sc. degree in electronic information technology from the Macau University of Science and Technology, in 2008, the M.Sc. degree in e-commerce technology and the Ph.D. degree in software engineering from the University of Macau, in 2010 and 2013, respectively. From 2014 to 2015, she was a Postdoctoral Fellow with the Department of Computer and Information Science, University of Macau. She is currently an Assistant Professor with the Faculty of Information Technology, Macau University of Science and Technology. Her research interests include digital multimedia processing, digital watermarking, multimedia forensics, tampering detection and self-recovery, acoustic processing and diagnosis, and deep learning techniques and applications.

**HAI CHEN** received the B.S. degree in electrical engineering from the Shaanxi University of Science and Technology, Xi'an, China, in 1995, the M.S. degree in logistics engineering from Beijing Wuzi University, Beijing, China, in 2008, and the Ph.D. degree in computer science and engineering from the Macau University of Science and Technology, Macau, in 2019. Since 2007, she has been an Associate Professor with the Faculty of Information Technology, Beijing Normal University, Zhuhai, China. Her research interests include signal processing, speech recognition, machine learning, deep learning, and the Internet of Things.

**JIANQING LI** (Senior Member, IEEE) received the Ph.D. degree from the Beijing University of Posts and Telecommunications, Beijing, China, in 1999. From 2000 to 2002, he was a Visiting Professor with the Information and Communications University, Daejeon, South Korea. From 2002 to 2004, he was a Research Fellow with Nanyang Technological University, Singapore. He joined the Macau University of Science and Technology, Macau, in 2004, where he is currently a Professor. His research interests include wireless networks, fiber sensors, and the Internet of Things.